# Iris Recognition Using One-Dimensional Signal Analysis

Edmundo Daniel Hoyle Delgado[1], Raul Queiroz Feitosa[2], Antonio Petraglia[3]

[1] Universidade Federal de Rio de Janeiro, Rio de Janeiro - RJ, Brasil, edhoyle@pads.ufrj.br
[2] Universidade Federal de Rio de Janeiro, Rio de Janeiro - RJ, Brasil, petra@pads.ufrj.br
[3] Pontifícia Universidade Católica do Rio de Janeiro, Rio de Janeiro - RJ, Brasil, raul@ele.puc-rio.br

**Abstract:** This paper introduces a new, low computational complexity approach for iris recognition function that is able to cope with occlusion, caused by eyelids and eyelashes. The method has been extensively tested using 2500 images, achieving correct recognition rate of 100%, rate recognition of 99.992% and equal error rate of 0.01%.

**Keywords:** Biometric, iris recognition, wavelet transform, zero crossings representation, dissimilarity function.

## 1. INTRODUCTION

Personal identification techniques using biometrics characteristics have been studied with the purpose of preventing fraud, falsification of documents, patents and terrorism. Various approaches exploiting physical traits such as fingerprints, voice tone and timber, face, hand geometry and retina patterns have been proposed [1]. Systems based on the iris structure have the potential of playing a major role. The iris contains a group of characteristics that makes it one of the safest biometric features for identification. It is clearly visible, which eases its capture, and is already entirely formed by the first year of one's life and remains unchanged. On the other hand, parts of the iris images are usually occluded by eyelashes and eyelids [2].

John Daugman [3] was the pioneer in this field, developing mathematical algorithms which allowed the iris' image to be digitally encoded. Next to the Daugman model, the methods proposed by Wildes [4] and Boles [5], [6] are the most often cited in the literature. These approaches, however, have certain limitations. The Wildes' method works in verification mode only, whereas the Boles' method does not take occlusion into consideration

This paper proposes an extension to Boles` method that it less sensitive to occlusion than in its original formulation. Extensive experimental analyses are carried out on the *CASIA Iris Database* [7] to verify its identification performance.

## 2. IDENTIFICATION THROUGH IRIS IMAGES

The process of human identification based on the structure of the iris may be divided in five main steps: image acquisition, segmentation, normalization, representation, matching.

The first step is responsible for capturing the iris images. The acquired image must be segmented in the second step. Here, both the inner edge of the iris at the pupil and the outer edge at the sclera are located (see Figure 1). In the normalization step a geometric transformation is applied to the region comprised between the inner and outer iris edges resulting in a rectangular image, as illustrated in Figure 2.

In the next step the information contained in the normalized image is represented in a more compact form to save computer storage space. The representation retains the distinctive iris features so as to permit identification. However, for security reasons, the representation is such that the reconstruction of the original image from it is impossible.

The final step, called matching, consists in determining whether different iris images belong or not to the same subject. This is usually done in two different operation modes. In the verification mode the system checks if a claimed identity and the biometric data are consistent (positive) or not (negative). In this mode the provided biometric data undergoes steps 1 to 4 and the resulting representation is compared with samples recorded in a database associated to the declared subject. The identification mode is about searching the system database for the record that best matches a given biometric data, aiming at establishing the subject's identity. In both modes, matching operations are performed upon representations rather than on the original images. This paper focuses henceforth on representation and matching, assuming that an appropriate solution for acquisition, segmentation, normalization steps has been already provided.

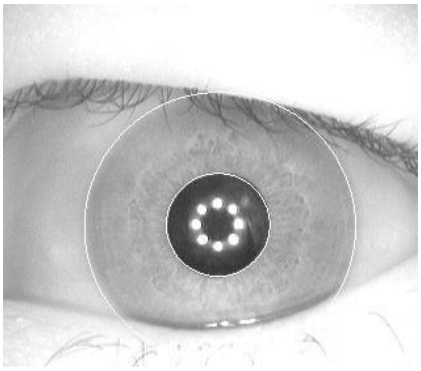

Fig. 1. Eye image with segmented pupil and iris.

## 3. BOLES` METHOD

This section describes succinctly how representation and matching are performed according to Boles proposal.

### *3.1. Representation*

The starting point for the iris representation is the information of pixel intensities in the normalized iris image, as shown in Figure 2. Each row of the normalized image forms a vector which is later treated as a single period sample of a one-dimensional periodic signal.

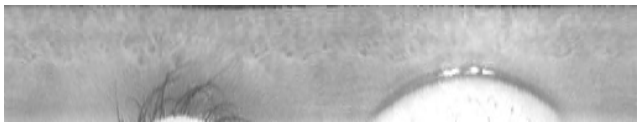

Fig. 2. Normalized iris' image with occlusion from Figure 1.

A dyadic wavelet transform is applied to each row vector and decomposing it in different resolution levels. As the information in the highest resolution levels is generally very much affected by noise, they is discarded for the following analysis. The authors concluded experimentally that the fourth, fifth and sixth levels are enough to generate a good representation.

The zero crossings of the dyadic wavelet transform of the row signals are determined for each of the 3 levels mentioned above. These points occur where there is an abrupt change in the signal amplitude. Figure 3 shows an example of a zero crossing representation of the wavelet transform of a given row of the normalized image.

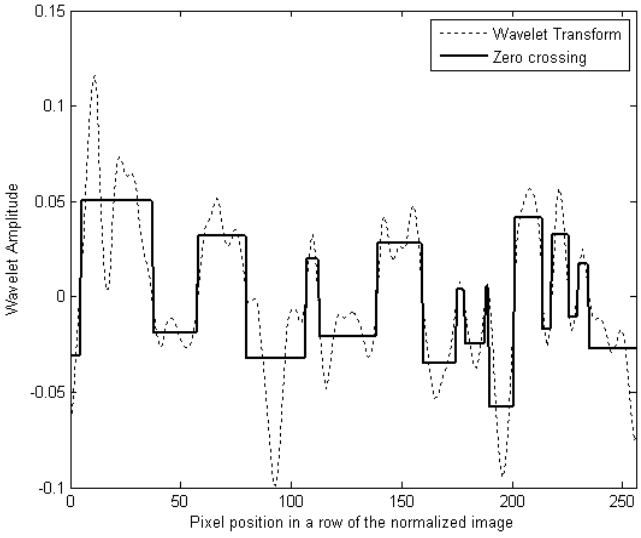


Fig. 3. Wavelet transform and its zero-crossing representation.

Once the zero crossings have been located, the average value between each two consecutive zero crossing points in the wavelet outcome is computed. Accordingly, working with normalized images with 16 rows and 512 columns, in the original Boles paper, the iris is represented by a matrix having 48×256 elements [5]. In this paper, on the other hand, the iris is represented by a matrix of 48×512 elements. We shall return to this issue in Section 4.

### *3.2. Matching*

To compute the dissimilarity between two irises, their zero crossing representations are compared. Boles propose four functions to measure the dissimilarity between the signals [5]. Hereafter only the dissimilarity measure defined by

$$d_{jm}(f,g) = 1 - \frac{\sum_{n=0}^{N-1} Z_j f(n) \cdot Z_j g(n+m)}{\| Z_j f \| \| Z_j g \|} \qquad (1)$$

is considered, since it provides the best performance in the experiments conducted within this work. In the above equation, $d_{jm}(f,g)$ denotes the dissimilarity of irises f and g associated to the j-th row of their representation matrices for a displacement m, the vectors $Z_jf$ and $Z_jg$ are the j-th row of the zero crossing representations respectively of irises f and g, N is the number of elements of $Z_jf$ and $Z_jg$, and m,n $\in$ [ 0 N-1]. The symbol "|| ||" denotes the vector norm operation. Note that $d_{jm}(f,g)$ is equal to 1 minus the correlation coefficient between $Z_jf(n)$ and $Z_jg(n)$. Thus the dissimilarity $d_{jm}(f,g)$ may take values between 0 and 2, whereby 0 corresponds to a perfect match.

Equation (1) is computed for each row of the representation matrices. For normalized images with 16 rows and working with 3 resolution levels, this will return 48 values, whose mean is taken as the dissimilarity ($D_m$) between irises f and g, for a given value of m.

It is important to notice that m in (1) represents shifts of the second signal. Varying m in (1) from 0 to N-1 yields N dissimilarity values ($D_m$). The overall dissimilarity D between irises f and g is given by

$$D = \min_m (D_m) \qquad (2)$$

## 4. METHODOLOGY

This section describes the proposed approach to deal with occlusion. It is assumed henceforth that the occlusion areas in the normalized images were determined in a previous step, and zero value was attributed to the corresponding pixels. The basic idea consists in restricting the computation of dissimilarity to the values of the wavelet transforms not influenced by occlusion. Since the wavelet transform is a neighborhood operation, it is affected by occlusion over a range the goes beyond the pixels directly under occlusion. It includes the occluded pixels themselves and the pixels lying in a neighborhood of size *w*, where *w* is the width of the wavelet kernel. The wavelet used was taken from the Gaussian derivatives family (first derivative of the Gaussian probability density function).

Let us now take the *j*-th row of both normalized images and compute their wavelet transforms. They are illustrated in Figure 4 by their respective dotted and dashed lines. These two curves differ from each other only in the region not affected by occlusion. The other (solid) curve in Figure 4, is produced by zeroing any of the earlier curves only where they differ. Hence, to ignore pixels under occlusion, the similarity analysis should be limited to the non zero values of this third curve.

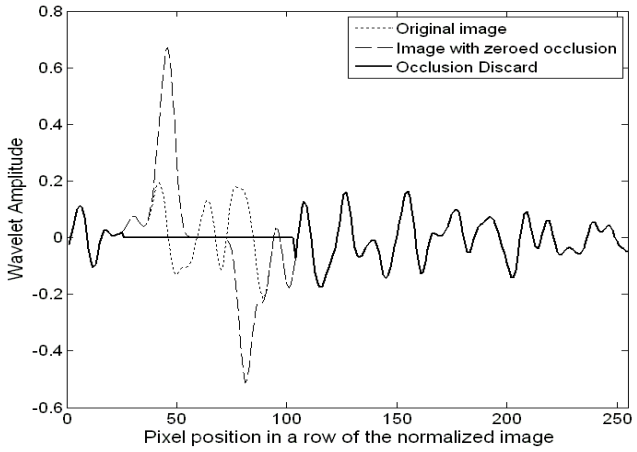


Fig. 4. Wavelet transforms.

This idea is explained in more formal terms as follows. Let $Z_j f$ and $Z_j g$ be the zero crossing representation produced by the wavelet transforms of the j-th row of a normalized image, such as the one shown in Figure 2. Similarly $Z'_j f$ and $Z'_j g$ are the zero crossing representations of the same row but with zeros over occluded pixels. In addition, let $Z^*_j f$ and $Z^*_j g$ denote the vectors defined as

$$Z_j^* f(n)\begin{cases} = Z_j f(n), \ for\ Z_j f(n) = Z_j' f(n) \\ = 0 \quad otherwise \end{cases} \tag{3}$$

and

$$Z_j^* g(n)\begin{cases} = Z_j g(n), \ for\ Z_j g(n) = Z_j' g(n) \\ = 0 \quad otherwise \end{cases} \tag{4}$$

Hence, Z*jf and Z*jg derive from Zjf and Zjg by setting to zero the elements affected by occlusion. Now, let zjf and zjg be the vectors formed only by the elements of Z*jf and Z*jg, respectively, for which Z*jf(n)≠0 and Z*jg(n+m) ≠0. The length M of zjf and zjg will depend not only on the number and position of the pixels under occlusion in both images being compared, but also on m. Clearly, for a given value of m the information in Zjf and Zjg relative to non occluded areas is totally contained in zjf and zjg. As a result, the dissimilarity Boles function can be computed only on zjf and zjg. A simple manipulation leads to the conclusion that

$$\frac{\sum_{p=0}^{M-1} z_j f(p) z_j g(p)}{\left\| z_j f \right\| \left\| z_j g \right\|} = \frac{\sum_{n=0}^{N-1} Z_j^* f(n) Z_j^* g(n+m)}{\left\| Z_j^* f \right\| \left\| Z_j^* g \right\|} \tag{5}$$

and hence, the dissimilarity function to cope with occlusion can be written as

$$d_{jm}(f,g) = 1 - \frac{\sum_{n=0}^{N-1} Z_j^* f(n) Z_j^* g(n+m)}{\| Z_j^* f \| \ \| Z_j^* g \|} \tag{6}$$

The dissimilarity of two irises f and g is given in original Boles' method [5] by the plain average of the 48 values to each row of the zero crossing representation matrices. This work proposes the use of a weighted mean, instead of the simple mean, whereby the weights are given by the number of non zeroed values in $Z^*_j f(n)$ and $Z^*_j g(n)$, according to

$$D_m = \sum_{j=1}^{48} d_{jm}(f,g) \times k_j \Big/ \sum_{j=1}^{48} k_j \tag{7}$$

where $d_{jm}(f,g)$ is given by (6) and $k_j$ is the number of non zeroed values in the j-th row of the zero crossing representations of both images.

## 5. PERFORMANCE ANALYSIS

To assess the performance of the proposed method, experiments were conducted using 2500 irises images from *CASIA Iris database*. The experiments were carried out in two modes: verification mode (one-to-one matching) and identification mode (one-to-many matching). In verification mode, the equal error rate (EER) is used in the performance evaluations. The EER is the point where the false match rate and the false nonmatch rate are equal in value. The smaller the EER is, the better the algorithm. In identification mode, the algorithm is measured by correct recognition rate (CRR), which is the ratio of the number of samples being correctly classified to the total number of test samples. Figure 5 shows the histograms of the overall dissimilarity for positives and negatives produced by the original Boles method, as well as by the proposed method.

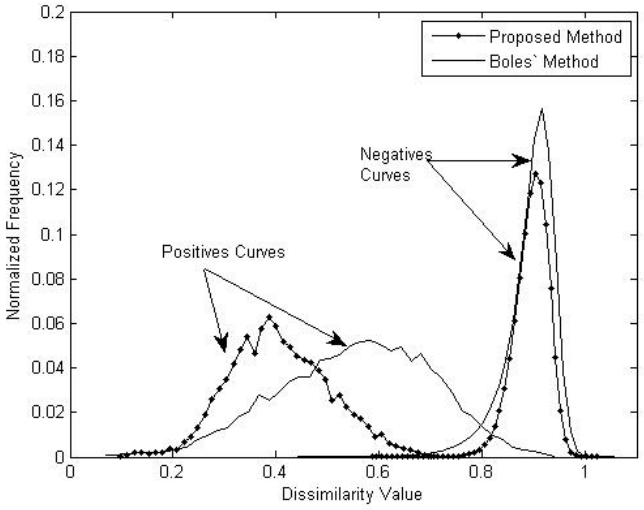


Fig. 5. Histograms of positives and negatives.

The superiority of the proposed method can be seen by observing the area of overlap between the curves for positives and negatives. As this area increases, so does the occurrence of either false positives or false negatives. In Figure 5 the overlap area for the curves of the Boles` method is larger than that for the proposed method, which indicates that the former less accurate. The number of false positives and false negatives depends on the acceptance threshold for the dissimilarity value. For example, in high security applications where the consequences of a false positive are very serious, it is recommended to work with a low acceptance threshold. On the other hand, for applications where the inconvenience caused by a false

negative is a major concern, a comparatively higher acceptance threshold may be appropriate. The CCR and EER values computed from the experiments. are displayed in Table 1. Results reported by other competing techniques are also shown.

Table 1. Experimental Results and Comparisons[a].

| Author | CCR (%) | EER (%) | Number of Images |
|---|---|---|---|
| Ma et al. [8] | 100 | 0.07 | 2255 |
| Monro et al. [9] | 100 | $2.59 \times 10^{-4}$ | 2156 |
| Roy et al. [10] | 99.81 | 0.13 | 756 |
| Poursaberi et al. [11] | 99.31 | 0.2687 | 756 |
| Daugman [3] | 100[b] | 0.08[b] | 2255[b] |
| Wildes [4] | ----- | 1.76[b] | 2255[b] |
| Boles et al. [6] | 96.60[c] | 4.2[c] | 2500[c] |
| Proposed | 100 | 0.01 | 2500 |

[a]All methods employ *CASIA Iris Database*.
[b]Results published in [8].
[c]Results produced in this paper with Boles´ method.

## 6. CONCLUSIONS

This work presented a low complexity iris recognition technique, which is based on one-dimensional analysis of iris images. Experiments conducted on images from the *CASIA Iris Database* indicated that the proposed approach significantly improves the recognition performance. The efficiency of the method depends on how accurately the occlusion areas are delineated in the input image. Extensively tested, the algorithm proved its ability to cope with occlusion, and showed highly accurate recognition performance. A comparison with alternative iris recognition techniques was also shown.

## 7. REFERENCES


[1] S. Nanavati, M. Thieme, and R. Nanavati, Biometrics: Identity Verification in a Networked World, John Wiley & Sohns, 2002.

[2] H. Proença and L. A. Alexandre, **"**A Method for the Identification of Noisy Regions in Normalized Iris Images**,"** *18th International Conference on Pattern Recognition*, vol. 4, p. 405 – 408, 2006.

[3] J. Daugman, "How Iris Recognition Works," *IEEE Transactions on circuits and systems for video technology*, vol. 14, n.1, p.21-31, Jan 2004

[4] R. P. Wildes, "Iris recognition: an emerging biometric technology," *Proceedings of the IEEE,* vol. 85, n. 9, p. 1348 – 1363, Sept 1997

[5] W.W. Boles "A security System Based on Human Iris Identification Using Wavelet Transform," *First International Conference on Knowledge-Based intelligent Electronic System,* Adelaide, Australia Editor, L.C. Jan, pp. 533-541, May 1997.

[6] W.W. Boles and B. Boashash "A human Identification Technique using images of the Iris and wavelet transform", *IEEE transactions on signal processing*, 1185-1188, April 1998.

[7] CASIA Iris Database, Center for Biometrics and Security Research http://www.cbsr.ia.ac.cn/IrisDatabase.htm, 6 Aug. 2008.

[8] L. Ma, T. Tan, Y. Wang, and D. Zhang, "Efficient Iris Recognition by Characterizing Key Local Variations," *IEEE Trans. Image Processing*, vol. 13, pp. 739-750, 2004.

[9] D. M. Monro, S. Rakshit, and D. Zhang, "DCT-based iris recognition," *IEEE Trans. Pattern Analysis and Machine Intelligence*, vol. 29, no. 4, pp. 586–595, Apr. 2007.

[10] K. Roy and P. Bhattacharya, "Optimal Features Subset Selection and Classification for Iris Recognition," *EURASIP Journal on Image and Video Processing*, vol. 2008, Article ID 743103, 20 pages, 2007.

[11] A. Poursaberi and B. N. Araabi, "Iris Recognition for Partially Occluded Images: Methodology and Sensitivity Analysis," *EURASIP Journal on Advances in Signal Processing*, vol. 2007, Article ID 36751, 12 pages, 2006.